Multipartite nonlocality and boundary conditions in one-dimensional spin chains

Zhao-Yu Sun,[1,*] Mei Wang,[1] Yu-Yin Wu,[1] and Bin Guo[2]
[1]*School of Electrical and Electronic Engineering, Wuhan Polytechnic University, Wuhan 430023, China*
[2]*Department of Physics, Wuhan University of Technology, Wuhan 430070, China*

(Received 31 December 2018; revised manuscript received 24 February 2019; published 15 April 2019)

In quantum lattice models, in the large-N limit, boundary conditions have little effect upon local observables for sites in the centers of the lattices. In this paper, we will study the boundary effects upon multipartite nonlocality (a kind of multipartite quantum correlation associated with Bell-type inequalities) in one-dimensional finite-size spin chains, both for zero temperature and for finite temperatures. We define a quantity $\frac{\delta\mathcal{S}}{\mathcal{S}}$ to characterize the boundary effects, where $\mathcal{S}$ is a measure of global multipartite nonlocality of the entire lattice, and $\delta\mathcal{S}$ is the difference of the measure induced by changing the boundary conditions. We find $\frac{\delta\mathcal{S}}{\mathcal{S}}$ does not vanish in the large-N limit. Instead, at zero temperature, with the increase of N, $\frac{\delta\mathcal{S}}{\mathcal{S}}$ would increase steadily in the vicinity of the quantum phase transition point of the models, and converge to a nonzero constant in noncritical regions. It shows clearly that boundary effects generally exist, in the form of multipartite correlations, in long chains. The boundary effects are explained by the competition between the two orders of the models. In addition, based on these numerical results, we construct a Bell inequality, which is violated by chains with periodic (closed) boundary conditions and not violated by chains with open boundary conditions. Furthermore, we study $\frac{\delta\mathcal{S}_T}{\mathcal{S}_T}$ of finite-size chains at finite temperatures, and show that boundary effects survive in finite temperature regions.

DOI: 10.1103/PhysRevA.99.042323

I. INTRODUCTION

Quantum correlations play an important role in the fields of both quantum information and condensed-matter physics [1,2]. A wide range of progresses have been achieved for bipartite quantum correlations, such as quantum entanglement entropy [3]. Recently, the concepts of quantum correlations have been generalized into multipartite settings, i.e., multipartite correlations [4–8]. On the one hand, multipartite quantum correlation turns out to be an indispensable resource in scalable quantum computing, secret-sharing protocols, and quantum communication [2,9]. On the other hand, multipartite correlations can reveal more detailed structure of quantum correlations in many-body systems, thus offerring us a deeper understanding of condensed matters and quantum phase transitions [10–12].

Among various measures of quantum correlations, quantum nonlocality [13] has attracted much attention recently. A key feature of quantum nonlocality is that it can be detected by the violation of Bell-type inequalities in laboratory experiments [14]. Furthermore, it can be naturally generalized into multipartite settings, that is, multipartite nonlocality [15–21]. Nonlocality and Bell-type inequalities have been investigated in many low-dimensional models, including the Heisenberg chains [22,23], the Lipkin-Meshkov-Glick models [24], the Kitaev-Castelnovo-Chamon model [25], and many others [26–28]. It has been found that the Bell inequality is not violated in two-site subchains in these models, thus nonlocality is not observed. It is pointed out by Oliveira *et al.* [29] that in most one-dimensional translationally invariant models quantum nonlocality should not exist in the form of two-site (bipartite) nonlocality. A counterexample is found by Sun *et al.* [30]. Consequently, multipartite nonlocality has been used to describe quantum correlations in these models. It has been confirmed that in these chains quantum nonlocality indeed exists, i.e., in the form of multipartite nonlocality [11,12,26,26,31–33]. In addition, even genuine multipartite nonlocality has been observed in some models [33]. Furthermore, nonlocality has been used to characterize quantum phase transitions in one-dimensional infinite-size quantum models [12,23–27,31,32]. Since global multipartite nonlocality in the entire infinite-size lattice is untractable, partial nonlocality in n-site subchains has been investigated in these studies.

In a quite recent paper [34], it is realized that in some situations, when a many-body system manifests genuine multipartite nonlocality, then there cannot be arbitrarily high partial nonlocality in its subsystem. This indicates that analysis of partial nonlocality in n-site subchains may not always lead to the true information of the global nonlocality of the entire lattice. Thereby, it is quite valuable to investigate directly the global nonlocality of the entire lattice. Since an explicit calculation of the global nonlocality in the infinite-size chains is impossible, it would be feasible to investigate the global nonlocality in finite-size chains, combined with some finite-size scaling analysis.

It needs to be mentioned that, for finite-size chains, a physical issue emerges naturally, i.e., the boundary conditions.

Boundary conditions play an important role in numerical simulations of quantum lattices [35–38]. The most widely used boundary conditions are the open boundary conditions and the periodic (closed) boundary conditions. For instance, a finite-size chain with an open boundary condition usually

*Corresponding author: sunzhaoyu2000@qq.com

has a larger energy gap than one with a periodic boundary condition. Thus, although periodic boundary conditions are strongly preferable in analytical solutions, one tends to adopt open boundary conditions in numerical simulations (such as in density-matrix renormalization-group algorithm [39]). In addition, some "artificial" boundary conditions have also been proposed to simulate one-dimensional lattices, such as the twisted boundary condition [40], the smooth boundary condition [41], and the infinite boundary condition [42]. This *freedom* of choosing various boundary conditions is based upon a general conclusion that, if the length of the chains is large enough, changing boundary conditions does not affect local physical properties for sites in the centers of the chains.

However, when considering global multipartite nonlocality which spreads in all chains, is it still safe to use this *freedom* to adopt some favorite boundary conditions in our simulations? How do the boundary conditions affect the global multipartite nonlocality in the chains? These questions remain unknown. We would like mention that the global multipartite nonlocality of several finite-size chains (with periodic boundary conditions) has been investigated [11,33], and the boundary effects have not been analyzed.

In this paper, we study multipartite nonlocality and boundary conditions in one-dimensional finite-size transverse-field Ising chains. We characterize the boundary effects upon multipartite nonlocality of the models with a quantity $\frac{\delta\mathcal{S}}{\mathcal{S}}$, where $\mathcal{S}$ is the measure of the global multipartite nonlocality of the entire lattice, and $\delta\mathcal{S}$ is the boundary-induced difference of the measure. We find that $\frac{\delta\mathcal{S}}{\mathcal{S}}$ remains nonzero for any finite magnetic field. Thereby, changing boundary conditions affects the global multipartite correlations in the chains (with local reduced density matrices nearly unaffected). Especially, with the increase of the length of the chains, we observe two kinds of scaling behavior for $\frac{\delta\mathcal{S}}{\mathcal{S}}$; that is, it converges to a constant in noncritical regions, while increasing steadily in critical regions. Furthermore, in the critical regions, we construct a special Bell inequality, which is violated by the closed chains and not violated by the open chains. We offer a physical explanation for the boundary effects by the competition between the two orders of the models, and investigate the boundary effects in the chains at finite temperatures.

This paper is organized as follows. In Sec. II, the concepts of multipartite nonlocality and Bell-type inequalities are briefly introduced. In Sec. III, multipartite nonlocality and boundary effects in finite-size transverse-field Ising chains are investigated. A summary and some discussions are given in Sec. IV.

II. MULTIPARTITE NONLOCALITY AND BELL-TYPE INEQUALITIES

The concept of multipartite nonlocality can be introduced in several alternative ways [6,19,21,43]. A widely used definition is based on the so-called g-grouping models. Let us consider a model which consists of N sites. Suppose it can be divided into (at most) g subgroups, and only sites in the same subgroup can communicate with each other. Then it is called a g-grouping model. For instance, one may use $\{1|1|1|1\}$, $\{1|1|2\}$, $\{2|2\}$, and $\{4\}$ to denote a four-grouping model, a three-grouping model, a two-grouping model, and a one-grouping model, respectively, with the total sites $N = 4$. For an N-site quantum state $\hat{\rho}$, if its correlations can be reproduced by an N-grouping model $\{1|1|...|1\}$, we say that $\hat{\rho}$ does not contain any form of multipartite nonlocality. Instead, if its correlations can be reproduced only by a one-grouping model $\{N\}$, we say that $\hat{\rho}$ contains genuine multipartite nonlocality. Thereby, according to the structure of multipartite nonlocality in $\hat{\rho}$, we are able to classify $\hat{\rho}$ into different classes.

In practice, the structure of multipartite nonlocality of the state $\hat{\rho}$ can be detected with Bell-type inequalities. First, on every site, we need to define two operators $\hat{m}_j = \vec{a}_j \cdot \vec{\sigma}$ and $\hat{m}'_j = \vec{a}'_j \cdot \vec{\sigma}$, where $j = 1, 2, \dots, N$ labels the sites, $\vec{a}_j$ and $\vec{a}'_j$ are unit vectors on site j, and $\vec{\sigma}$ is just the spin vector. Then the N-site Mermin-Svetlichny operators are defined in a recursive way as [15,16,18–20]

$$\hat{M}_{[1\dots N]} = \tfrac{1}{2}\hat{M}_{[1\dots N-1]} \otimes (\hat{m}_N + \hat{m}'_N) + \tfrac{1}{2}\hat{M}'_{[1\dots N-1]} \otimes (\hat{m}_N - \hat{m}'_N), \tag{1}$$

$$\hat{M}'_{[1\dots N]} = \tfrac{1}{2}\hat{M}'_{[1\dots N-1]} \otimes (\hat{m}'_N + \hat{m}_N) + \tfrac{1}{2}\hat{M}_{[1\dots N-1]} \otimes (\hat{m}'_N - \hat{m}_N), \tag{2}$$

with $\hat{M}_1 = \hat{m}_1$ and $\hat{M}'_1 = \hat{m}'_1$. To proceed, let us further define the operator $\hat{S}$ as

$$\hat{S}_{[1\dots N]} = \frac{1}{\sqrt{2}}\big(\hat{M}_{[1\dots N]} + \hat{M}'_{[1\dots N]}\big). \tag{3}$$

Then for any N-site quantum state the correlations of which can be reproduced by some g-grouping model, one can prove that the following Bell-type inequality holds [19]:

$$\mathcal{S} = \begin{cases} \max_{\{\boldsymbol{a}\}} \big\langle \hat{M}_{[1\dots N]} \big\rangle \leqslant 2^{\frac{N-g}{2}}, & \text{for N-g even,} \\ \max_{\{\boldsymbol{a}\}} \big\langle \hat{S}_{[1\dots N]} \big\rangle \leqslant 2^{\frac{N-g}{2}}, & \text{for N-g odd,} \end{cases} \tag{4}$$

where $\{\boldsymbol{a}\}$ denotes the set of the $2N$ unit vectors, and $\langle\cdot\rangle$ denotes the expectation value $\mathrm{Tr}(\hat{\rho}\,\cdot)$ for the state $\hat{\rho}$. For a given N, one can see that $g = N, N-1, \dots, 2$ labels a series of Bell-type inequalities. If the g-labeled inequality is violated, one says that some $g-1$(or less)-grouping model is needed to reproduce the multipartite nonlocality in the state. For instance, the lowest-order Bell inequality is $\mathcal{S} \leqslant 1$ (corresponding to $g = N$). If it is not violated, no multipartite nonlocality is observed. On the other hand, the highest-order Bell inequality is $\mathcal{S} \leqslant 2^{\frac{N-2}{2}}$ (corresponding to $g = 2$). If it is violated, some one-grouping model is needed to reproduce the quantum correlations in the state. In the language of multipartite nonlocality, we say that the state contains genuine multipartite nonlocality.

The quantity $\mathcal{S}$ is called the Bell correlation function, or simply the nonlocality measure. In practice, when N is large, we are interested in the qualitative behavior of multipartite nonlocality in the chains, rather than the specific value of g. Thereby, we will ignore the parity of $N - g$ in Eq. (4) and just consider an even $N - g$. As we show in this paper, the functional behavior of $\mathcal{S}$ is quite informative in capturing the trend of the global multipartite nonlocality in the transverse-field Ising chains.

III. MAIN RESULTS

A. Models and solution

In order to investigate boundary effects upon multipartite nonlocality in one-dimensional quantum lattices, we consider one of the most simple one-dimensional models, that is, the N-site transverse-field Ising model described by

$$\hat{H} = -\sum_{i=1}^{N-1} \hat{\sigma}_i^z \hat{\sigma}_{i+1}^z - \lambda \sum_{i=1}^{N} \hat{\sigma}_i^x - J\hat{\sigma}_N^z \hat{\sigma}_1^z, \tag{5}$$

where $\hat{\sigma}_i^{x,z}$ are Pauli matrices on site i, and λ is the strength of the magnetic field in the x direction. The last term $J\hat{\sigma}_N^z\hat{\sigma}_1^z$ describes the boundary condition of the chains. For an open boundary condition, we set $J = 0$, while for a closed (periodic) boundary condition we set $J = 1$. When the magnetic field vanishes ($\lambda = 0$), the ground states of the chains are Greenberger-Horne-Zeilinger (GHZ) states, regardless of the boundary conditions or the size of the chains. When λ is strong enough, the model will be in a polarized state along the x direction. A second-order quantum phase transition occurs at $\lambda_c = 1$ in thermodynamic limit $N \to +\infty$.

We investigate the boundary effects on multipartite nonlocality of finite-size chains. The ground-state wave functions of the chains with the open boundary condition and the closed boundary condition will be denoted as $|\psi_{\text{open}}\rangle$ and $|\psi_{\text{closed}}\rangle$, respectively. When $N \leqslant 14$, the ground states are solved exactly. For $N > 14$, the ground states will be expressed as matrix product states (MPSs) with the ALPS package [44]. Then the global nonlocality measure $\mathcal{S}$ for finite-size chains will be figured out with an MPS-based numerical optimization algorithm, where some techniques can be found in Ref. [12]. The results for the ground states are presented in Secs. III B–III D, and a physical explanation of the boundary effects is given in Sec. III E. Furthermore, at finite temperatures, the thermal states of the chains are described by $\hat{\rho}_T = e^{-\beta\hat{H}}$, with β the inverse temperature. We solve $\hat{\rho}_T$ exactly for $N \leqslant 12$, and investigate the boundary effects on the thermal-state nonlocality of finite-size chains in Sec. III F.

B. Basic properties of multipartite nonlocality

In Fig. 1, we illustrate the nonlocality measure $\mathcal{S}$ as a function of the magnetic field λ in finite-size chains with the open boundary condition [Fig. 1(a)] and the closed boundary condition [Fig. 1(b)]. One can see that for the two situations the trends of the $\mathcal{S}(\lambda)$ curves are very similar to each other. Thereby, first, open chains are used to describe the basic picture of the global multipartite nonlocality in the models. Based on that, the boundary effects are analyzed in the next subsection.

For open chains [Fig. 1(a)], when the magnetic field is strong, i.e., $\lambda = 2$, the nonlocality measure is slightly larger than 1 for finite N. According to the Bell-type inequalities in Eq. (4), only the lowest hierarchy of multipartite nonlocality is observed. In addition, in the limit $\lambda \to \infty$, it is expected that the nonlocality measure approaches 1 and multipartite nonlocality vanishes. Thus, we turn our attention to the low-field regions by considering $\lambda = 0.1$. For $N = 2, 4, 6, 8, 10, 12,$ and 14, the nonlocality measure is 1.401, 2.81, 5.614, 11.21, 22.4, 44.75, and 89.38, respectively. Thereby, according to Eq. (4), for any given N, the highest-order Bell-type inequality is violated, and genuine multipartite nonlocality is observed.

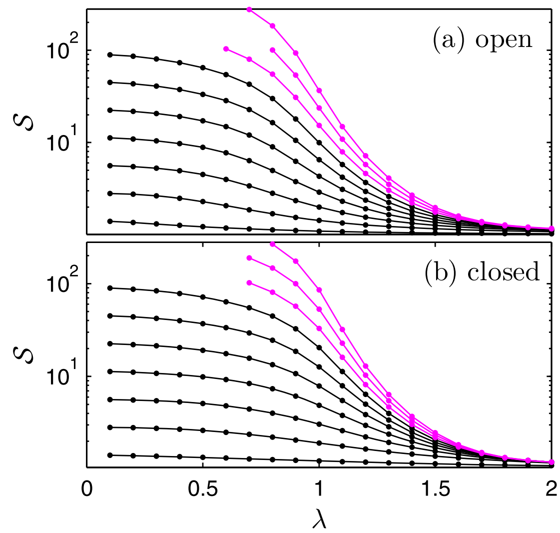

FIG. 1. Nonlocality measure $\mathcal{S}$ as a function of the magnetic field λ for finite-size transverse-field Ising chains with (a) open boundary conditions and (b) closed boundary conditions for various N. In both figures, from bottom to top, the curves correspond to $N = 2, 4, 6, 8, \ldots, 20$. The figures indicate that with the increase of λ the ground states of the models change from genuine multipartite nonlocal states to classical states gradually.

When the magnetic field increases from zero to ∞, the nonlocality measure decreases gradually, and the ground states transform gradually from states with genuine multipartite nonlocality to states with no nonlocality. In addition, in Fig. 1(a) one can see that the first derivative of the nonlocality measure, i.e., $\frac{\partial \mathcal{S}}{\partial \lambda}$, is relatively small for $\lambda = 0.1$ and 2, and is relatively large in the vicinity of the quantum phase transition point $\lambda_c = 1$. Furthermore, with the increase of N, the $\mathcal{S}(\lambda)$ curve becomes steeper in the vicinity of λ_c, and it is expected that, in the limit $N \to \infty$, $\frac{\partial \mathcal{S}}{\partial \lambda}$ diverges at λ_c. Thus, the quantum phase transition at $\lambda_c = 1$ in the (infinite-size) models is accompanied by dramatic changes of the global multipartite nonlocality of the ground states.

C. Boundary effects on multipartite nonlocality

We now discuss the boundary effects on the ground states. In Fig. 2(c), we show the nonlocality measure $\mathcal{S}$ as a function of the magnetic field λ for both boundary conditions with $N = 12$. For comparison purposes, we also show the ground-state energy $E = \langle\psi|\hat{H}|\psi\rangle$ and the magnetization $M_x = \langle\psi|\sum_{i=1}^{N}\hat{\sigma}_i^x|\psi\rangle$ in Figs. 2(a) and 2(b), respectively. One can see that in the critical regions ($\lambda \approx 1$) the nonlocality measure $\mathcal{S}$ and the magnetization M_x suffer some effect from the boundary conditions, and in the noncritical regions ($\lambda \approx 0$ and 2) they suffer very little influence from the boundary conditions. Generally speaking, the ground states are affected

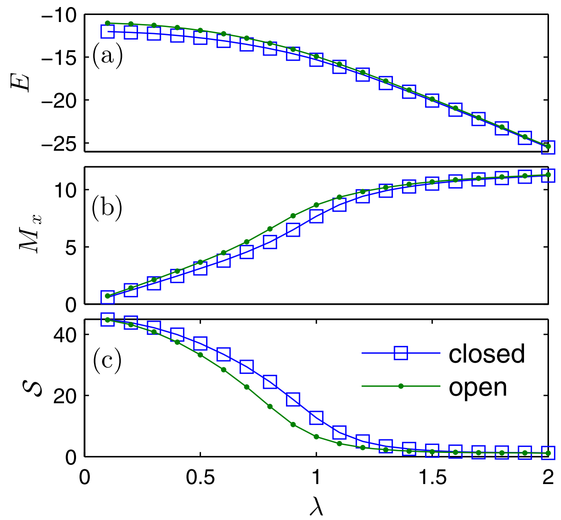

FIG. 2. (a) Ground-state energy E, (b) magnetization M_x, and (c) nonlocality measure $\mathcal{S}$ as a function of the magnetic field λ for finite-size transverse-field Ising chains with $N = 12$. Squares and dots correspond to closed chains and open chains, respectively. The figures show that in the critical regions $\lambda \approx 1$ the ground states are affected strongly by boundary conditions.

strongly by boundary conditions in the critical regions, and weakly in noncritical regions.[1]

In order to characterize the boundary effects quantitatively, we define a quantity $\frac{\delta F}{F}$ as

$$\frac{\delta F}{F} = \left|\frac{F_{\text{closed}} - F_{\text{open}}}{F_{\text{open}}}\right|, \qquad (6)$$

with $F = E, M_x, \mathcal{S}$. The subscripts denote the corresponding boundary conditions under which the observables are figured out, i.e., $F_{\text{open}} = \langle\psi_{\text{open}}|\hat{F}|\psi_{\text{open}}\rangle$. If boundary conditions have rather small effect upon the ground states, i.e., $|\psi_{\text{closed}}\rangle \approx |\psi_{\text{open}}\rangle$, $\frac{\delta F}{F}$ is very small. On the other hand, if boundary conditions indeed have considerable effects upon the ground states, some $\frac{\delta F_0}{F_0}$ are relatively large. This physical observable F_0 offers us a perspective to understand the boundary effects in the models.

In Fig. 3 we illustrate the results of $\frac{\delta F}{F}$ as a function of N, with the chains under the critical field $\lambda_c = 1$. We find that with the increase of N both $\frac{\delta E}{E}$ and $\frac{\delta M_x}{M_x}$ decrease gradually. The energy and the magnetization are just the summation of local physical quantities, i.e., $\langle\hat{\sigma}_i^z\hat{\sigma}_{i+1}^z\rangle$ and $\langle\hat{\sigma}_i^x\rangle$. This demonstrates that with the increase of the length of the chains the boundary effects upon these local physical quantities become weaker gradually. However, in Fig. 3(c), we observe that $\frac{\delta\mathcal{S}}{\mathcal{S}}$ shows a steady enhancement as a function of N. Thereby, multipartite nonlocality suffers a considerable influence from

[1]In Fig. 2(a), when the magnetic field is very weak, the energy E shows a considerable effect from the boundary conditions. In fact, when $\lambda = 0$, the open chain and the closed chain share the same ground state, i.e., the GHZ state. Thus, the energy difference between the two chains comes from the boundary term $-J\hat{\sigma}_N^z\hat{\sigma}_1^z$ of the Hamiltonian in Eq. (5), rather than the discrepancy between the ground states $|\psi_{\text{open}}\rangle$ and $|\psi_{\text{closed}}\rangle$.

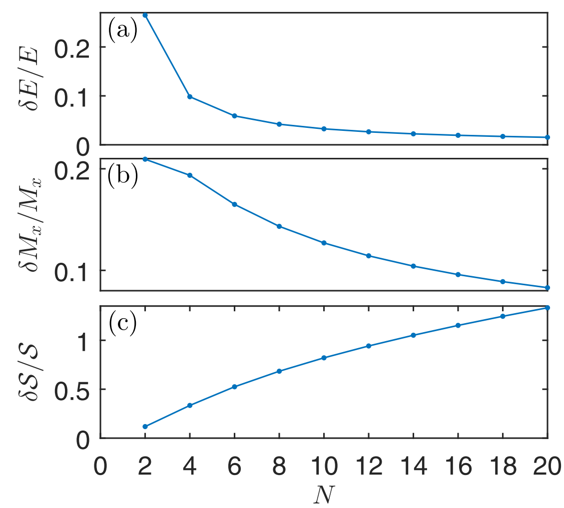

FIG. 3. Boundary effects on (a) ground-state energy, (b) magnetization, and (c) nonlocality measure, respectively, as a function of the length N of the chains with the magnetic field $\lambda = 1$. The definition of $\frac{\delta F}{F}$ is shown in Eq. (6). With the increase of N, the boundary effects upon the energy and the magnetization become weak, and the boundary effect upon multipartite nonlocality becomes strong.

the boundary conditions for large N. The weakening of $\frac{\delta E}{E}$ and $\frac{\delta M_x}{M_x}$ and the enhancement of $\frac{\delta\mathcal{S}}{\mathcal{S}}$ reveal that, in long chains, while boundary conditions have weak (if any) influence upon local observables, they have a strong influence upon multipartite quantum correlations of the chains.

In Fig. 3 we have only considered $\lambda_c = 1$. For $\lambda < 1$, our results on $\frac{\delta\mathcal{S}}{\mathcal{S}}$ are shown in Fig. 4(a). First, when $\lambda = 0$ (which is not shown in the figure), both $|\psi_{\text{open}}\rangle$ and $|\psi_{\text{closed}}\rangle$ are GHZ states, thus it is clear that $\frac{\delta\mathcal{S}}{\mathcal{S}} = 0$. However, for a small finite field $\lambda = 0.2$, we find that $\frac{\delta\mathcal{S}}{\mathcal{S}}$ is not zero.

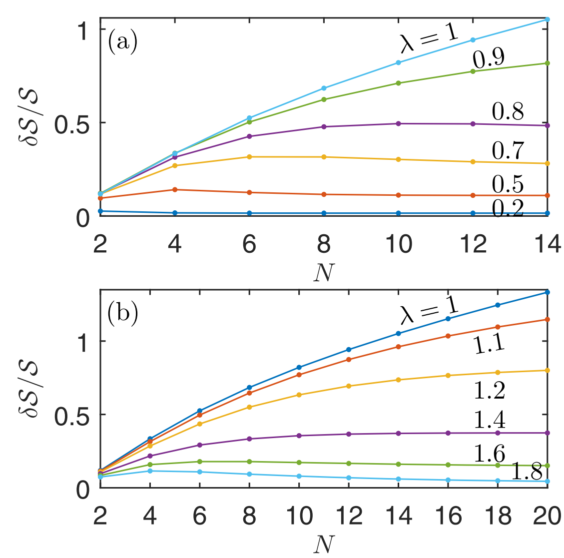

FIG. 4. Scaling behavior of the boundary effect upon nonlocality measure for various magnetic fields λ. $\lambda = 1$ is the critical point for the (infinite-size) models.

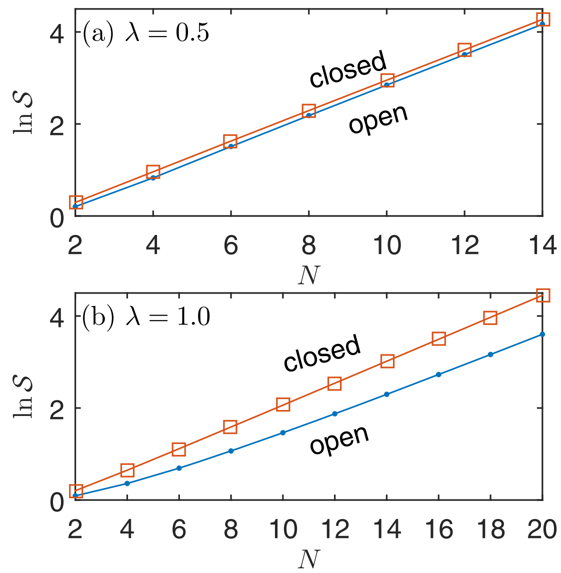

FIG. 5. Logarithm of nonlocality measure as a function of the length of the chains, with the magnetic field (a) $\lambda = 0.5$ and (b) $\lambda = 1.0$. Squares and dots correspond to closed chains and open chains, respectively.

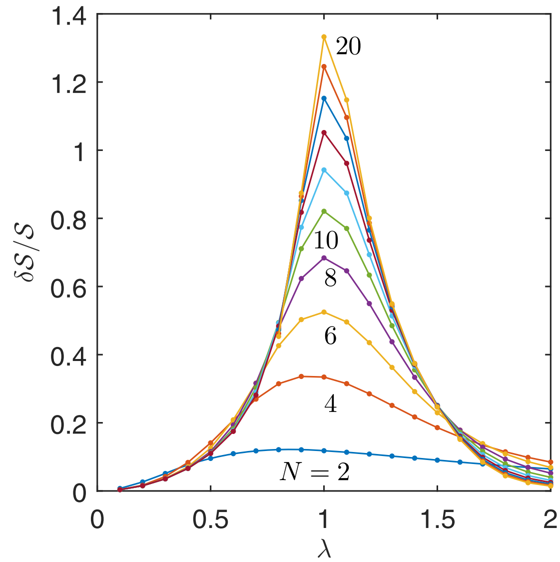

FIG. 6. Boundary effect upon nonlocality measure as a function of the magnetic field λ for various N. From bottom to top, the curves correspond to finite-size chains with $N = 2, 4, 6, 8, \dots, 20$. $\lambda = 1$ is the critical point for the (infinite-size) models.

Instead, with the increase of N, $\frac{\delta\mathcal{S}}{\mathcal{S}}$ converges to a nonzero constant 0.01534. This indicates that the boundary conditions always have an impact upon the ground states for any finite N. For $\lambda = 0.5$, we find that $\frac{\delta\mathcal{S}}{\mathcal{S}}$ converges to a slightly larger value, i.e., 0.1099. When the magnetic field approaches the critical regions, that is, $\lambda \approx 1$, $\frac{\delta\mathcal{S}}{\mathcal{S}}$ does not converge any more. Instead, it increases steadily as a function of N. The results for when the field crosses the critical point, that is, $\lambda > 1$, are shown in Fig. 4(b). One can see that when the field is strong enough $\frac{\delta\mathcal{S}}{\mathcal{S}}$ again converges to a constant gradually, with the increase of N.

It is clear that the size dependence of $\frac{\delta\mathcal{S}}{\mathcal{S}}$ in the noncritical regions is quite different from that in the critical regions. These behaviors can be explained as follows. First, the nonlocality measure $\mathcal{S}$ scales exponentially with the increase of N. In Fig. 5(a), we show $\ln \mathcal{S}$ as a function of N for both boundary conditions, with $\lambda = 0.5$. One can see that the two lines are parallel to each other. In other words, they can be fitted by

$$\ln \mathcal{S}_{\text{closed}} = k_1 N + b_1,$$
$$\ln \mathcal{S}_{\text{open}} = k_2 N + b_2, \tag{7}$$

with $k_1 = k_2$ and $b_1 \neq b_2$. Thereby, it is straightforward to prove that

$$\frac{\delta\mathcal{S}}{\mathcal{S}} = \frac{e^{kN+b_1} - e^{kN+b_2}}{e^{kN+b_2}} = e^{\Delta b} - 1, \tag{8}$$

where $\Delta b = b_1 - b_2$ results from the boundary effect. Consequently, $\frac{\delta\mathcal{S}}{\mathcal{S}}$ has little dependence upon the size N of the chains. This is why $\frac{\delta\mathcal{S}}{\mathcal{S}}$ converges to a constant in noncritical regions in Fig. 4. When $\Delta b = 0$, it is clear that $\frac{\delta\mathcal{S}}{\mathcal{S}} = e^0 - 1 = 0$, which is just the situation for $\lambda = 0$, i.e., the GHZ state.

For critical regions, we show in Fig. 4 that $\frac{\delta\mathcal{S}}{\mathcal{S}}$ does not converge. Thereby, the behavior cannot be explained by Eq. (8), and we need to take the boundary effect on k into consideration, i.e., $\Delta k = k_1 - k_2 \neq 0$ [see Fig. 5(b)]. Then we have

$$\frac{\delta\mathcal{S}}{\mathcal{S}} = \frac{e^{k_1 N+b_1} - e^{k_2 N+b_2}}{e^{k_2 N+b_2}} = e^{\Delta kN+\Delta b} - 1, \tag{9}$$

where both Δb and Δk result from the boundary effects. In Eq. (9), if ΔkN is small enough,[2] we have $e^{\Delta kN} \approx 1 + \Delta kN$. Then Eq. (9) reduces to

$$\frac{\delta\mathcal{S}}{\mathcal{S}} \approx \Delta k e^{\Delta b} N + e^{\Delta b} - 1. \tag{10}$$

Thus, the quasilinear growth of $\frac{\delta\mathcal{S}}{\mathcal{S}}$ for $\lambda_c = 1$ in Fig. 4 is also explained.

Finally, in Fig. 6, we illustrate $\frac{\delta\mathcal{S}}{\mathcal{S}}$ as a function of the magnetic field λ for various N. When N is very small, $\frac{\delta\mathcal{S}}{\mathcal{S}}$ shows a broad and round peak in the vicinity of the phase transition point $\lambda_c = 1$. With the increase of N, the peak becomes very sharp. This shows clearly that when a phase transition indeed occurs (in systems with $N \to \infty$) boundary conditions have a sharp impact upon the global multipartite nonlocality of the ground states.

D. A Bell inequality for different boundaries

From Fig. 6 one can see that, under the conditions that (1) the chains are in the critical regions $\lambda \approx 1$ and (2) the length N is large enough, we have $\frac{\delta\mathcal{S}}{\mathcal{S}} > 1$, in other words,

$$\mathcal{S}_{\text{open}} < \tfrac{1}{2} \times \mathcal{S}_{\text{closed}}. \tag{11}$$

[2]The condition can be satisfied when Δk is nearly zero and N is finite.

Then it is straightforward to prove that the N-site Bell inequality

$$\mathcal{S}_{[1,\ldots,N]} \leqslant 2^{\frac{N-\lceil\zeta\rceil}{2}} \tag{12}$$

with

$$\zeta = N - 2\log_2 \mathcal{S}_{\text{closed}} \tag{13}$$

is violated by the N-site closed chains and not violated by the N-site open chains.

The proof is as follows. According to Eq. (13), we have

$$\mathcal{S}_{\text{closed}} = 2^{\frac{N-\zeta}{2}} > 2^{\frac{N-\lceil\zeta\rceil}{2}}, \tag{14}$$

where we have assumed $\zeta < \lceil\zeta\rceil$, without loss of generality. Thereby, Eq. (12) is violated in the closed chains.

Next, let us prove that the inequality is not violated in open chains. First, it is clear that

$$\zeta + 2 > \lceil\zeta\rceil.$$

Then it is clear that

$$2^{\frac{N-\zeta}{2}-1} < 2^{\frac{N-\lceil\zeta\rceil}{2}}. \tag{15}$$

Finally, according to Eqs. (11), (14), and (15), we have

$$\mathcal{S}_{\text{open}} < \tfrac{1}{2} \times \mathcal{S}_{\text{closed}} = \tfrac{1}{2} \times 2^{\frac{N-\zeta}{2}} < 2^{\frac{N-\lceil\zeta\rceil}{2}}. \tag{16}$$

Thus, Eq. (12) is not violated by open chains.

The violation and the nonviolation of the Bell inequality in closed chains and open chains, respectively, indicate that Bell-type inequalities offer us a tool to disclose the sharp discrepancy between the ground states of spin chains with different boundary conditions.

E. Physical explanation for boundary effects

We have considered only two types of boundary conditions in previous sections, that is, the closed (periodic) boundary conditions with $J = 1$ [see Eq. (5)] and the open boundary conditions with $J = 0$. In order to obtain a more intuitive understanding of the boundary effects, it may be helpful to consider the "intermediate boundary conditions" with $0 < J < 1$, and investigate what happens in the intermediate process between $J = 1$ and 0. First, let us consider the critical regions. In Fig. 7, we show the nonlocality measure $\mathcal{S}$ for chains with $N = 14$ and $\lambda = 1$, where the results for boundary parameter $0 < J < 1$ are marked as white dots. One can see that the nonlocality measure $\mathcal{S}$ is rather sensitive to the boundary parameter J. Especially, when J decreases from one to zero, the nonlocality measure $\mathcal{S}$ decreases steadily. This stable decline of $\mathcal{S}$ helps us to draw an intuitive picture of the possible origin of the boundary effects. First, in the Hamiltonian of Eq. (5), there is a clear competition between the ferromagnetic interaction term

$$\hat{H}_2 = -\sum_{i=1}^{N-1} \hat{\sigma}_i^z \hat{\sigma}_{i+1}^z - J\hat{\sigma}_N^z \hat{\sigma}_1^z$$

and the transverse-field term

$$\hat{H}_\lambda = -\lambda \sum_{i=1}^{N} \hat{\sigma}_i^x.$$

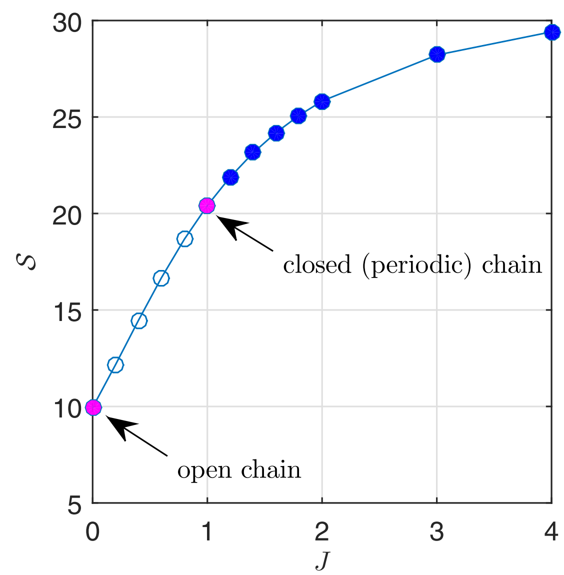

FIG. 7. Nonlocality measure $\mathcal{S}$ as a function of the general boundary parameter J for finite-size transverse-field Ising chains with $\lambda = 1$ and $N = 14$. J describes the boundary condition of the model in Eq. (5).

The $\hat{H}_2$ term favors the GHZ-type ground state, which carries a large value of $\mathcal{S}$, and the $\hat{H}_\lambda$ term favors the polarized state, which carries a small value of $\mathcal{S}$. Thereby, generally speaking, increasing the transverse field λ tends to weaken the nonlocality measure $\mathcal{S}$ (also see Fig. 1). Then we analyze the effect of the boundary parameter J on the competition between $\hat{H}_2$ and $\hat{H}_\lambda$. When J decreases from one to zero, one can see that the ferromagnetic interaction term $\hat{H}_2$ is slightly weakened. Then, because of the competition between $\hat{H}_2$ and $\hat{H}_\lambda$, any weakening of $\hat{H}_2$ implies the relative enhancement of the transverse-field term $\hat{H}_\lambda$. Consequently, one may say that the effective magnetic field λ is slightly increased. According to Fig. 1, the increase of λ finally weakens the nonlocality measure $\mathcal{S}$. Thereby, we have explained the general boundary effects, that is, the decrease of the boundary parameter J weakens the nonlocality measure $\mathcal{S}$. On the other hand, one may deduce that the increase of the boundary parameter J enhances the nonlocality measure $\mathcal{S}$. To check the theory, we have also calculated the nonlocality measure for $J > 1$ and the results are marked as blue dots in Fig. 7. It is clear that our theory is confirmed.

The boundary conditions with $0 < J < 1$ and $J > 1$ are quite artificial. However, they offer strong support for our physical picture of the boundary effects. We conclude that the boundary effects in the transverse-field Ising chains are originated from the competition between the two orders in the models.

Furthermore, let us explain why the boundary effects are strong in the critical regions and weak in the noncritical regions (see Fig. 6). According to the $\mathcal{S}(\lambda)$ curves in Fig. 1, the nonlocality measure $\mathcal{S}$ is very sensitive to the change of the magnetic field λ in the critical regions, and not sensitive in the noncritical regions. In other words, $\frac{d\mathcal{S}}{d\lambda}$ is large for $\lambda \approx 1$ and is nearly zero for $\lambda \approx 0$ and $\gg 1$. Thereby, when the boundary parameter J decreases from one to zero the effective

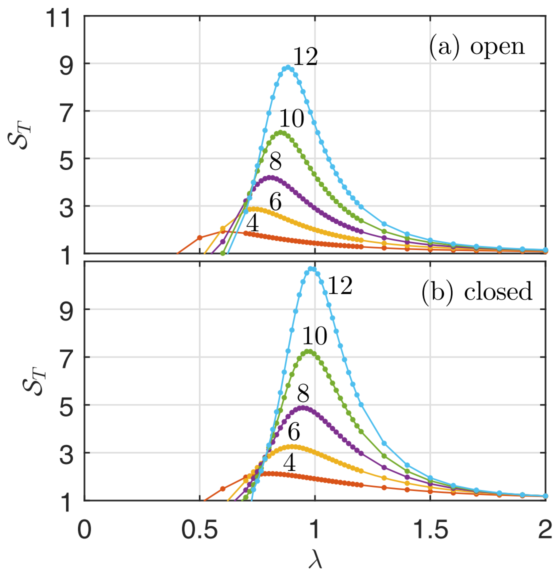

FIG. 8. Nonlocality measure $\mathcal{S}_T$ as a function of the magnetic field λ for finite-size transverse-field Ising chains at finite temperature $T = 0.05$ with (a) open boundary conditions and (b) closed boundary conditions for various N. In both figures, from bottom to top, the curves correspond to $N = 4, 6, 8, 10, 12$. $\lambda = 1$ is the critical point for the (infinite-size) models.

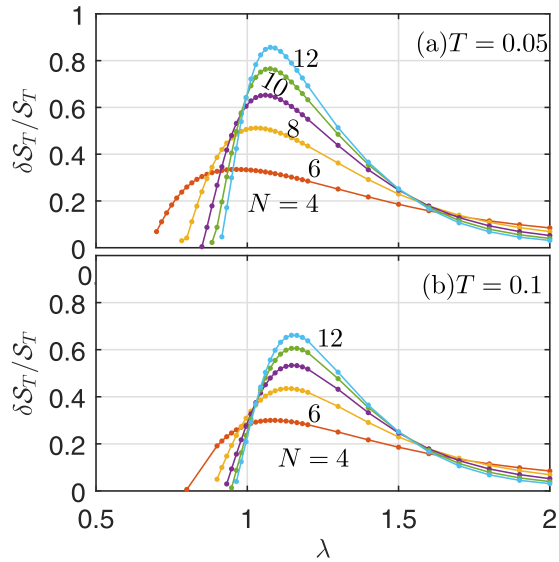

FIG. 9. Boundary effect upon nonlocality measure as a function of the magnetic field λ at finite temperatures (a) $T = 0.05$ and (b) $T = 0.1$ for various N. From bottom to top, the curves correspond to finite-size chains with $N = 4, 6, 8, 10, 12$. Higher temperatures induce a decrease of the maximum value of $\delta\mathcal{S}_T/\mathcal{S}_T$ and a deviation of the peak point away from the critical point $\lambda = 1$ gradually.

magnetic field increases; in the critical regions, it is expected that a considerable change in the nonlocality measure $\mathcal{S}$ is observed. In other words, a strong boundary effect emerges. On the other hand, in the regions far away from $\lambda = 1$, when the effective magnetic field increases, it is expected that the nonlocality measure $\mathcal{S}$ shows little change. Thereby, a weak boundary effect emerges. In fact, one can see that the $\frac{\delta\mathcal{S}}{\mathcal{S}}(\lambda)$ curves in Fig. 6 capture the main trend of the derivative of $\mathcal{S}(\lambda)$ curves in Fig. 1, which is quite consistent with our theory.

F. Boundary effects at finite temperatures

In this subsection, we consider boundary effects on multipartite nonlocality of the finite-size chains at finite temperatures. For such a purpose, we need to study the nonlocality measure for the thermal state $\hat{\rho}_T = \frac{e^{-\beta\hat{H}}}{\mathrm{tr}(e^{-\beta\hat{H}})}$, with $\beta = \frac{1}{k_B T}$. In this paper, we set $k_B = 1$ and denote the thermal-state nonlocality measure as $\mathcal{S}_T = \mathcal{S}(\hat{\rho}_T)$. We mention that for the closed chains the thermal-state nonlocality measure has been studied in Ref. [11], where the boundary effects have not been considered.

First, we describe the basic properties of the nonlocality measure $\mathcal{S}_T$ both for the open chains and for the closed chains. The results for $T = 0.05$ are presented in Fig. 8. A striking feature is that the measure $\mathcal{S}_T$ is no longer a monotonic function of the magnetic field λ. Instead, at finite temperatures, $\mathcal{S}_T$ shows a round peak in the middle-field regions. In addition, one can see that with the increase of the length of the chains the position of the peak approaches the critical point $\lambda = 1$ gradually for both boundary conditions. Thus, in the large-N limit, the multipartite nonlocality of finite-size chains presents a peak point in the low-temperature critical regions. The direct reason for the emergence of the peak is that, in the low-field regions, the value of the nonlocality measure reduces drastically at finite temperatures. The underlying mechanism is as follows. For $\lambda = 0$, as we have shown, the ground states of the chains are GHZ states and thus are double degenerate. For a small λ, the ground states are also of GHZ type and are nearly double degenerate. Thereby, even at very low temperature, the first excited state plays a role in the thermal state $\hat{\rho}_T$, thus destroying the quantum correlations. Therefore, at zero temperature and finite temperatures, the chains show quite different features in the low-field regions. We mention that similar behavior has been observed in the global quantum discord at finite temperatures [45].

We now obtain a rough evaluation of the boundary effects by comparing the open chains in Fig. 8(a) and the closed chains in Fig. 8(b). Our first observation is that cutting the edge of the chains (by changing the boundary term from closed chains to open chains) weakens the nonlocality measure $\mathcal{S}_T$, which is consistent with the zero-temperature behavior. In addition, for the closed chain with $N = 12$, the peak position of the nonlocality measure $\mathcal{S}_T$ is about $\lambda = 0.98$, very close to the critical point $\lambda = 1$. For the open chain with $N = 12$, however, one can see that the peak position is just about $\lambda = 0.88$. Thereby, boundary conditions affect both the peak value and the peak position of the $\mathcal{S}_T(\lambda)$ curves at finite temperatures.

In order to reveal the boundary effects intuitively, we resort to the quantity $\frac{\delta\mathcal{S}_T}{\mathcal{S}_T}$ defined in Eq. (6). We will illustrate $\frac{\delta\mathcal{S}_T}{\mathcal{S}_T}$ as a function of both the magnetic field λ and the temperature T.

In Fig. 9, we have illustrated the $\frac{\delta\mathcal{S}_T}{\mathcal{S}_T}(\lambda)$ curves at the temperatures $T = 0.05$ and 0.1 for various N, where a round peak is observed in the middle-field regions. One can see that for $T = 0$ (Fig. 6), 0.05 [Fig. 9(a)], and 1 [Fig. 9(b)] the

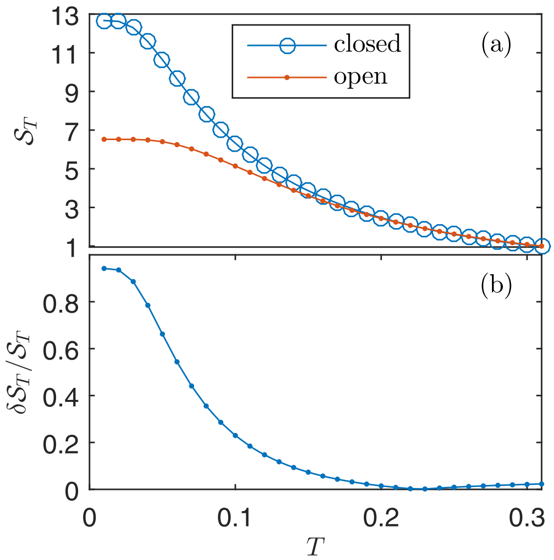

FIG. 10. (a) Nonlocality measure $\mathcal{S}_T$ as a function of the temperature T both for the open chain and for the closed chain with $N = 12$ and $\lambda = 1$. (b) Boundary effect upon nonlocality measure as a function of the temperature T for the finite-size chains with $N = 12$ and $\lambda = 1$.

peak position for $N = 12$ chains is about $\lambda \approx 1$, 1.08, and 1.15, respectively. Thus, with the increase of T, the peak point tends to deviate away from the critical point $\lambda = 1$ gradually. Moreover, we turn our attention to the peak value of the $\frac{\delta\mathcal{S}_T}{\mathcal{S}_T}(\lambda)$ curves. On the one hand, it is clear that even at finite temperatures increasing the size N of the chains enhances the peak value. On the other hand, at $T = 0$, 0.05, and 1, the peak value for $N = 12$ chains is about $\frac{\delta\mathcal{S}_T}{\mathcal{S}_T} \approx 0.94$, 0.86, and 0.66, respectively. Thus, enhancing the temperatures tends to weaken the boundary effects.

Let us conclude our analysis by considering $\frac{\delta\mathcal{S}_T}{\mathcal{S}_T}$ as a function of the temperature T for some fixed magnetic field. For such a purpose, we will consider only the magnetic field $\lambda = 1$, under which the chains show the strongest boundary effects at zero temperature (Fig. 6). Our results are shown in Fig. 10. One can see that, with the increase of the temperature T, $\mathcal{S}_T$ decreases steadily for both boundary conditions [Fig. 10(a)]. Especially, for $T \geqslant 0.31$ (which is not shown in the figure), $\mathcal{S}_T$ is smaller than 1 for both boundary conditions, thus no Bell-type inequality is violated. In Fig. 10(b), we illustrate $\frac{\delta\mathcal{S}_T}{\mathcal{S}_T}$ as a function of the temperature T. For $T \approx 0$, one can see that $\frac{\delta\mathcal{S}_T}{\mathcal{S}_T}$ shows some kind of thermal robustness against the increase of the temperatures. Then, for $0.02 \leqslant T \leqslant 0.23$, $\frac{\delta\mathcal{S}_T}{\mathcal{S}_T}$ vanishes gradually. For $T > 0.23$, $\frac{\delta\mathcal{S}_T}{\mathcal{S}_T}$ shows a low degree of revival. However, since the value for $\mathcal{S}_T$ is quite small in the high-temperature regions, this revival may not have any actual observable effect in experiments.

Our main observations are as follows. First, the boundary effects can be observed not just in the ground states but also at finite low temperatures. Second, in the large-N limit, $\frac{\delta\mathcal{S}_T}{\mathcal{S}_T}$ shows a peak in the vicinity of the critical point $\lambda = 1$ at low temperatures, indicating the quantum phase transition of the models. With the increase of T, the peak value decreases, and the peak position deviates away from the critical point $\lambda = 1$ gradually.

IV. SUMMARY AND DISCUSSIONS

In this paper, we have studied global multipartite nonlocality and boundary conditions in the finite-size transverse-field Ising model. Our first observation is that, in the low-field regions, the ground state of the model contains genuine multipartite nonlocality. We mention that for the same model with infinite size genuine multipartite nonlocality has not been detected in previous studies by investigating partial nonlocality in n-site subchains [12,31]. Thereby, genuine multipartite nonlocality in spin chains also presents the complementarity feature which was recently proposed by Sami *et al.* in no-signaling (Bell) nonlocal theories; that is, when a system has genuine multipartite nonlocality, then there cannot be arbitrarily high nonlocality in its subsystem [34]. Our results show clearly that analysis of partial nonlocality in n-site subchains does not always lead to the truth about the global nonlocality of the entire lattice. Thereby, it may be valuable to research the global nonlocality in the models which have been characterized by partial nonlocality in previous studies [23–26,31,32].

Then we have paid our attention to the boundary effects on all chains by defining a quantity $\frac{\delta F}{F}$ with $F = E, M_x, \mathcal{S}$, where the total energy E and the total magnetization M_x are the summation of local observables, and $\mathcal{S}$ measures the global multipartite nonlocality of the chains. δF is the increment of the measure induced by changing the boundary conditions. We find that with the increase of N both $\frac{\delta E}{E}$ and $\frac{\delta M_x}{M_x}$ vanish gradually. This indicates that in the large-N limit $|\psi_{\text{closed}}\rangle$ and $|\psi_{\text{open}}\rangle$ share the same local observables for most of the sites in the chains. On the other hand, we find that $\frac{\delta\mathcal{S}}{\mathcal{S}}$ does not vanish in the large-N limit. This indicates that the multipartite correlations in $|\psi_{\text{closed}}\rangle$ and $|\psi_{\text{open}}\rangle$ are different. These results can help us to draw an interesting physical picture about the boundary effects in the one-dimensional transverse-field Ising chains; that is, in the large-N limit, cutting a one-dimensional closed chain (a ring) into a one-dimensional open chain affects the global multipartite correlations in the lattices, with most of the local reduced density matrices unchanged.

Moreover, with the increase of N, we find that $\frac{\delta\mathcal{S}}{\mathcal{S}}$ converges to a constant in noncritical regions, while increasing steadily in critical regions. Based upon the exponential scaling of the nonlocality measure, we have offered a uniformed explanation of these results. These scaling behaviors also provide us an alternative method to characterize quantum phase transitions in low-dimensional quantum systems.

Based upon the numerical results, for chains in the critical regions, we have constructed a special Bell inequality in Eq. (12). The inequality is violated in the closed chains and not violated in the open chains, thus disclosing the sharp difference between the ground states of spin chains with different boundary conditions. Let us take the $N = 20$ chains with $\lambda = 1$ for instance, where $\mathcal{S}_{\text{open}} = 36.69$ and $\mathcal{S}_{\text{closed}} = 85.59$. Thereby, the Bell inequality in Eq. (12) is labeled by $\lceil\zeta\rceil = 8$. According to Eq. (4) and its interpretation, the correlations in the 20-site open chain may be reproduced by an eight-grouping model, such as $\{2|2|4|2|2|4|2|2\}$. However, since the inequality is violated by the closed chain, these eight-grouping models can never reproduce the correlations in the closed chain. Instead, seven(or less)-grouping models, such as {2|2|4|2|2|4|4}, are needed to reproduce the correlations in the closed chain. One can see that the sites in the closed chain are correlated in a more condensed form than in the open chain.

We have offered a physical explanation of the boundary effects. There is a clear competition between the ferromagnetic interaction term $\hat{H}_2$ and the transverse-field term $\hat{H}_\lambda$ of the transverse-field Ising chains, where the first term favors a high-$\mathcal{S}$ GHZ-type ground state, and the second term favors a low-$\mathcal{S}$ polarized state. Thereby, increasing (decreasing) the boundary parameter J enhances (weakens) the $\hat{H}_2$ term and thus weakens (enhances) the $\hat{H}_\lambda$ term relatively. Consequently, the effective magnetic field is weakened (enhanced), which finally leads to the enhancement (weakening) of the nonlocality measure $\mathcal{S}$. Under this picture, we further reveal that the $\frac{\delta\mathcal{S}}{\mathcal{S}}(\lambda)$ curves capture the main trend of the derivative of $\mathcal{S}(\lambda)$ curves of the models.

Finally, we have also studied the boundary effects of the models at finite temperatures. We find that the boundary effects can be observed not just in the ground states but also at finite low temperatures. In addition, at low temperatures, $\frac{\delta\mathcal{S}_T}{\mathcal{S}_T}$ for long chains shows a peak in the vicinity of the critical point $\lambda = 1$, thus indicating the quantum phase transition of the models. With the increase of T, the peak value decreases, and the peak position deviates away from the critical point $\lambda = 1$ gradually.

In this paper we have only considered the transverse-field Ising chains with open boundary conditions and the periodic (closed) boundary conditions. As we have mentioned, some other valuable boundary conditions (such as the twisted boundary condition, the smooth boundary condition, and the infinite boundary condition) have also been used widely [40–42]. In addition, there are many other interesting quantum lattices, such as the one-dimensional ladders. Especially, using various boundary conditions, an open ladder can be transformed into a cylinder or even a Mobius strip. It would be interesting to investigate global multipartite nonlocality and various boundary conditions in these lattices.

ACKNOWLEDGMENTS

Research was supported by the National Natural Science Foundation of China (Grants No. 11675124 and No. 11704295).

[1] G. Adesso, T. R. Bromley, and M. Cianciaruso, J. Phys. A: Math. Theor. **49**, 473001 (2016).
[2] G. D. Chiara and A. Sanpera, Rep. Prog. Phys. **81**, 074002 (2018).
[3] R. Horodecki, P. Horodecki, M. Horodecki, and K. Horodecki, Rev. Mod. Phys. **81**, 865 (2009).
[4] X. Wang, C. Zhang, Q. Chen, S. Yu, H. Yuan, and C. H. Oh, Phys. Rev. A **94**, 022110 (2016).
[5] S. Raeisi, P. Kurzyński, and D. Kaszlikowski, Phys. Rev. Lett. **114**, 200401 (2015).
[6] J.-D. Bancal, J. Barrett, N. Gisin, and S. Pironio, Phys. Rev. A **88**, 014102 (2013).
[7] F. Levi and F. Mintert, Phys. Rev. Lett. **110**, 150402 (2013).
[8] C. C. Rulli and M. S. Sarandy, Phys. Rev. A **84**, 042109 (2011).
[9] V. Scarani and N. Gisin, Phys. Rev. Lett. **87**, 117901 (2001).
[10] O. Göhne, G. Tóth, and H. J. Briegel, New J. Phys. **7**, 229 (2005).
[11] S. Campbell and M. Paternostro, Phys. Rev. A **82**, 042324 (2010).
[12] Z.-Y. Sun, B. Guo, and H.-L. Huang, Phys. Rev. A **92**, 022120 (2015).
[13] J. S. Bell, Physics Physique Fizika **1**, 195 (1964).
[14] M. Giustina, A. Mech, and A. Zeilinger, Nature (London) **497**, 227 (2013).
[15] D. Collins, N. Gisin, S. Popescu, D. Roberts, and V. Scarani, Phys. Rev. Lett. **88**, 170405 (2002).
[16] D. Collins, N. Gisin, N. Linden, S. Massar, and S. Popescu, Phys. Rev. Lett. **88**, 040404 (2002).
[17] J. Niset and N. J. Cerf, Phys. Rev. A **74**, 052103 (2006).
[18] Q. Y. He, E. G. Cavalcanti, M. D. Reid, and P. D. Drummond, Phys. Rev. Lett. **103**, 180402 (2009).
[19] J.-D. Bancal, C. Branciard, N. Gisin, and S. Pironio, Phys. Rev. Lett. **103**, 090503 (2009).
[20] J.-D. Bancal, N. Brunner, N. Gisin, and Y.-C. Liang, Phys. Rev. Lett. **106**, 020405 (2011).
[21] F. J. Curchod, N. Gisin, and Y.-C. Liang, Phys. Rev. A **91**, 012121 (2015).
[22] X. Wang and P. Zanardi, Phys. Lett. A **301**, 1 (2002).
[23] L. Justino and T. R. de Oliveira, Phys. Rev. A **85**, 052128 (2012).
[24] F. Altintas and R. Eryigit, Ann. Phys. **327**, 3084 (2012).
[25] D.-L. Deng, C. Wu, J.-L. Chen, S.-J. Gu, S. Yu, and C. H. Oh, Phys. Rev. A **86**, 032305 (2012).
[26] J. Batle and M. Casas, Phys. Rev. A **82**, 062101 (2010).
[27] B.-J. Chen, Z.-Y. Sun, H.-L. Huang, and B. Wang, Eur. Phys. J. B **87**, 282 (2014).
[28] H.-L. Huang, Z.-Y. Sun, and B. Wang, Eur. Phys. J. B **86**, 279 (2013).
[29] T. R. de Oliveira, A. Saguia, and M. S. Sarandy, Europhys. Lett. **100**, 60004 (2012).
[30] Z.-Y. Sun, Y.-Y. Wu, J. Xu, H.-L. Huang, B.-J. Chen, and B. Wang, Phys. Rev. A **88**, 054101 (2013).
[31] Z.-Y. Sun, Y.-Y. Wu, J. Xu, H.-L. Huang, B.-F. Zhan, B. Wang, and C.-B. Duan, Phys. Rev. A **89**, 022101 (2014).
[32] Z.-Y. Sun, S. Liu, H.-L. Huang, D. Zhang, Y.-Y. Wu, J. Xu, B.-F. Zhan, H.-G. Cheng, C.-B. Duan, and B. Wang, Phys. Rev. A **90**, 062129 (2014).
[33] Y. Dai, C. Zhang, W. You, Y. Dong, and C. H. Oh, Phys. Rev. A **96**, 012336 (2017).
[34] S. Sami, I. Chakrabarty, and A. Chaturvedi, Phys. Rev. A **96**, 022121 (2017).
[35] N. Shibata and C. Hotta, Phys. Rev. B **84**, 115116 (2011).
[36] S. R. White, Phys. Rev. B **48**, 10345 (1993).
[37] F. Verstraete, D. Porras, and J. I. Cirac, Phys. Rev. Lett. **93**, 227205 (2004).

[38] N. Laflorencie, E. S. Sørensen, M.-S. Chang, and I. Affleck, Phys. Rev. Lett. **96**, 100603 (2006).
[39] S. R. White, Phys. Rev. Lett. **69**, 2863 (1992).
[40] M. Thesberg and E. S. Sørensen, Phys. Rev. B **90**, 115117 (2014).
[41] M. Vekić and S. R. White, Phys. Rev. Lett. **71**, 4283 (1993).
[42] H. N. Phien, G. Vidal, and I. P. McCulloch, Phys. Rev. B **86**, 245107 (2012).
[43] E. G. Cavalcanti, Q. Y. He, M. D. Reid, and H. M. Wiseman, Phys. Rev. A **84**, 032115 (2011).
[44] B. Bauer, L. D. Carr, H. G. Evertz, A. Feiguin, J. Freire, S. Fuchs, L. Gamper, J. Gukelberger, E. Gull, S. Guertler, A. Hehn, R. Igarashi, S. V. Isakov, D. Koop, P. N. Ma, P. Mates, H. Matsuo, O. Parcollet, G. Pawłowski, J. D. Picon, L. Pollet, E. Santos, V. W. Scarola, U. Schollwöck, C. Silva, B. Surer, S. Todo, S. Trebst, M. Troyer, M. L. Wall, P. Werner, and S. Wessel, J. Stat. Mech.: Theor. Exp. (2011) P05001.
[45] S. Campbell, L. Mazzola, G. D. Chiara, T. J. G. Apollaro, F. Plastina, T. Busch, and M. Paternostro, New J. Phys. **15**, 043033 (2013).